Crushed aggregate response upon impact in dry and wet conditions

N. Petropoulos*, D. Johansson and E. Nordlund
Department of Civil, Environmental and Natural Resources Engineering, Luleå University of Technology, Sweden

*Corresponding author. Tel.: +46 725 430648;
E-mail address: nikolaos.petropoulos@ltu.se

Abstract

This paper presents results from a series of impact tests upon coarse-grained crushed aggregate. The material has been evaluated for two conditions, i.e. dry and wet (pendular state). Three main sets of test configurations were used with respect to compactive effort (low, medium and high) which was defined by the impact velocity of a drop hammer. Three accelerometers were installed in an impact machine to measure deceleration of the drop hammer and accelerations in the tested material at three different locations. The studied parameters were density, compaction, angle of repose, critical angle and particle size distribution. The results showed that the wet material gives larger density as well as critical angle. However, there was no discernible change in particle size distribution.

Keywords

Impact tests, granular material, aggregate, compaction, wet material, dry material

Introduction

In sub-level caving mining method, the production blasting is confined, i.e. the blasting is against pre-blasted or waste rock. The particle size distribution of the caved material has a wide range of fractions starting from fine material (size of millimeters) up to coarse fractions (size of meters). During the blast, there is only one degree of freedom for the blasted material, because at the sides of the blast there is only intact rock, which is perpendicular to the blasted material. The result of it is the compaction of the waste material which might affect its characteristics. This effect could be studied in similar manner as the effect of dynamic compaction on soil.

Soil compaction is necessary is numerous civil engineering areas. Among other techniques, dynamic compaction is extensively utilized in large engineering projects. This technique can be used as an analogue to the described tests in this paper. Dynamic compaction utilizes a heavy mass, weighing between 10 and 40 t, which is dropped from a height varying from 10 to 25 m to compact the area of interest. This method was first introduced by Menard & Broise, (1975) and it can be found that: i) in saturated soils the microbubbles affect the compressibility, ii) the repeated blows cause gradual liquefaction, iii) the permeability is affected by the fissures in the soil mass and iv) the presence of a thixotropic recovery as refered by Menard & Broise, (1975).

Numerous of laboratory tests and field tests have been conducted by, for example, Jessberger & Beine, (1981), Mayne & Jones, (1983), Womac, et al., (1989), Poran, et al., (1992), Thilakasiri, et al., (1996), Oshima & Takada, (1998), Merrifield & Davies, (2000), Gu & Lee, (2002) and Jafarzadeh, (2006) to investigate the behavior of soil masses under dynamic loading. In the majority of the tests, accelerometers and load cells have been used to assess the applied load by measuring the deceleration of the drop hammer on the soil sample and the recorded signals have been further used for calculations of the impact velocity and displacement of the impact surface. This type of tests have been used for very fine grained soil materials, i.e. sand, silt and clay.

Many researchers have tried to develop models for describing the behavior of soil masses under high-energy dynamic loading. The main source of developement and validation of these models has been extensive field data from case studies. Scott & Pearce, (1975) developed one-dimensional models which described the soil behavior under dynamic loading; the models considered materials such as ideal elastic unsaturated soil, elasto-plastic unsaturated soil, linear elastic soil in saturated state and saturated compactable soil. The results of the study showed that these models give reasonable results for very low impacts.

Mayne & Jones, (1983) carried out studies of the stress development as well as the effect of load duration on soil reaction due to dynamic loading. Their analysis of the field data was based on the assumption that a triagular pulse is applied on the surface of the impacted soil, i.e. a specific form of the applied force. Their method has been applied on different data sets from different literature sources. These included data sets from different test sites. It was observed that the model gave good predicions of the mangitude and duration of the stresses during impact. The model proposed by Scott & Pearce, (1975) has been found to be very limited in practical application as opposed to the model by Mayne & Jones, (1983) as stated by Chow, et al., (1992).

Chow, et al., (1990) and Chow, et al., (1992) proposed an analytical solution based on a modified one-dimensional wave equation model for pile-driving. They replaced the pile with a soil column extended to the depth of improvement. The surrounding soil is modelled with linear springs and linear dashpots. Additionally, an implicit finite element method was used to solve the equation of motion of the soil column. The model has been applied to field data from case studies. The measured quantity was the deceleration of the drop hammer which was used as input to their model. The results were shown to be in good aggrement with the recorded field data.

Extensive research, both field and laboratory tests, has been done on the study of the behavior of sandy and clayey soil masses subjected to dynamic compaction. However, the study of coarser soil materials is very limited, especially of coarse-grained aggregate as characterized by ASTM D2487-11, (2011). This paper presents the results from impact tests on coarse-grained aggregate. The measured quantities are density, angle of repose and compaction, although density and compaction are directly related to volumetric change of the tested material during the impact. Furthermore, the material has been tested under two different conditions, i.e. dry and with pendular water content, in this paper refered to as wet material.

Methodology

The apparatus in Figure 1 has been used to conduct the impact tests. The impact machine is a laboratory drop hammer-type machine which can be adjusted to various test set-ups. The parameters which can be adjusted are; the weight of the drop hammer and the impact velocity; In this paper, the impact velocity has been varied for the impact tests. This parameter defines the compactive effort applied on the surface of the tested material. The compactive effort describes the amount of energy supplied to the sample. The main parts of the impact machine are the drop hammer, the mold and the energy accumulator, i.e. elastic cords on both sides of the machine used to accelerate the drop hammer from its predefined drop height (1.5 m). The measurements, as mentioned before, included change in density of the material, angle of repose and compaction. The machine was equipped with 3 piezoelectric uniaxial accelerometers (PCB 350B03, 10 000g) which were connected with an amplifier and a logging unit. A detailed description of the impact machine can be found at Petropoulos, et al., (2017).

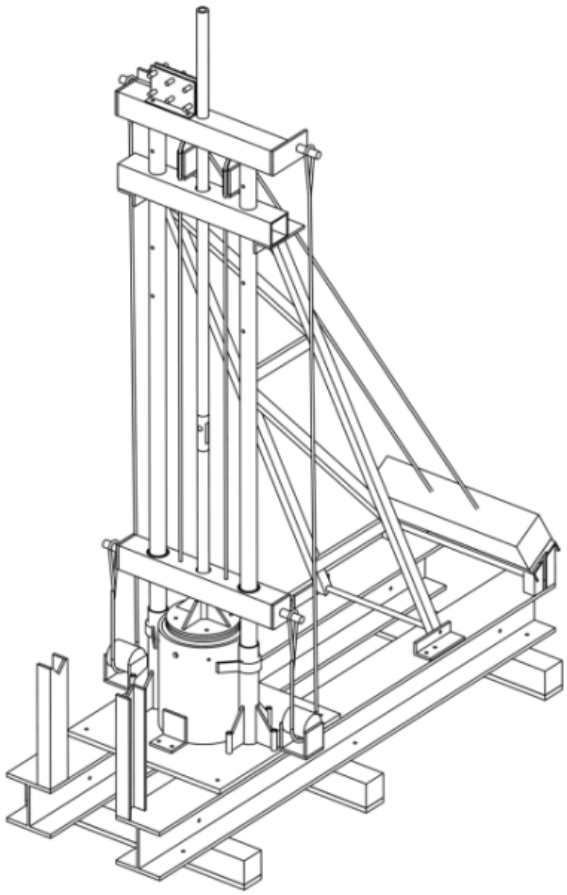

Figure 1: The impact machine

The locations of the installed sensors on the drop hammer and in the mold are shown in Figure 2 (all distances are in mm). Sensor (1) was installed on the drop hammer to measure its

deceleration. The other two sensors, i.e. (2) and (3), were installed in a telescopic system, i.e. the structure with pipes connected to the accelerometers, to measure acceleration/displacement. The telescopic system was located within the tested material. It was suspended in the mold during filling with the tested material to keep it at its predefined location. The thick line underneath the drop hammer denotes the surface of the tested sample and indicates the impact surface. The hatched area represents the coarse-grained material.

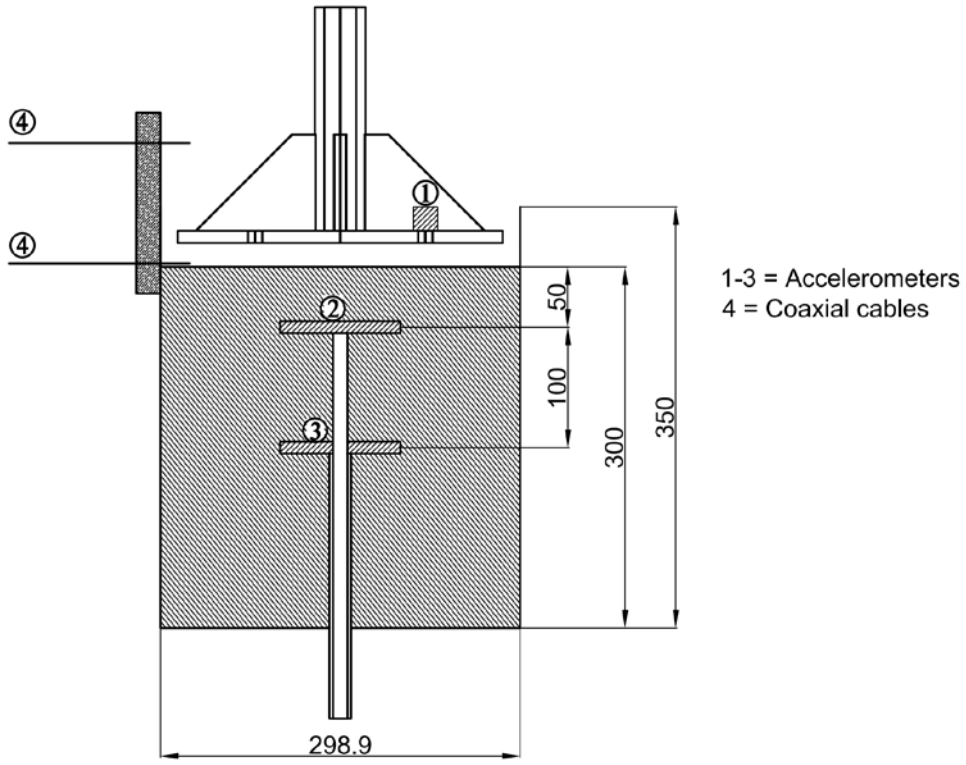

Figure 2: Section of the mold and location of the sensors (Petropoulos, et al., 2017)

The definition of the two different measurements was given as; (i) the recordings from the accelerometers were considered as dynamic measurements due to time dependency; (ii) the direct measurements of the displacement of the sensors before and after the impact were considered as static results. The analysis of the results was based on both dynamic and static measurements. The main difference between dynamic and static measurements was the time dependency. The dynamic measurements described the history of the acceleration while the static measurements described the residual displacement measured before and after the impact. The maximum displacement was calculated from the dynamic measurements while the residual displacement was based on the static measurements. The density and compaction were calculated based on the change in relative distance between the sensors, indicating volumetric change of the tested material.

Material preparation

The material has been evaluated at two different conditions, i.e. dry and wet. The material was dried in a laboratory oven according to ASTM D2216-10, (2010) and prepared for sieving in accordance with ASTM C136/C136M-14, (2014). The moisture content was 2.43±0.56 %. According to Newitt & Conwey-Jones, (1958) the saturation regime of the material with this water content is called pendular state. The physical description of this state is that liquid bridges are formed in between the particles. These liquid bridges influence some characteristics of the sample, i.e., cohesion, clustering and reduction of the friction coefficient. The particle size distribution of the tested material is shown in Figure 3. It should be noted that this figure shows the particle size distribution of the whole tested material and does not represent each individual test. The origin of the material is waste rock from the Kiirunavaara mine (LKAB) in northern Sweden. The material has passed through a crusher to fit the requirements of the impact machine. Consequently, the maximum particle size is less than 37.5 mm which is the maximum fragment size that the impact machine can host, in these tests the maximum fragment size was 32 mm.

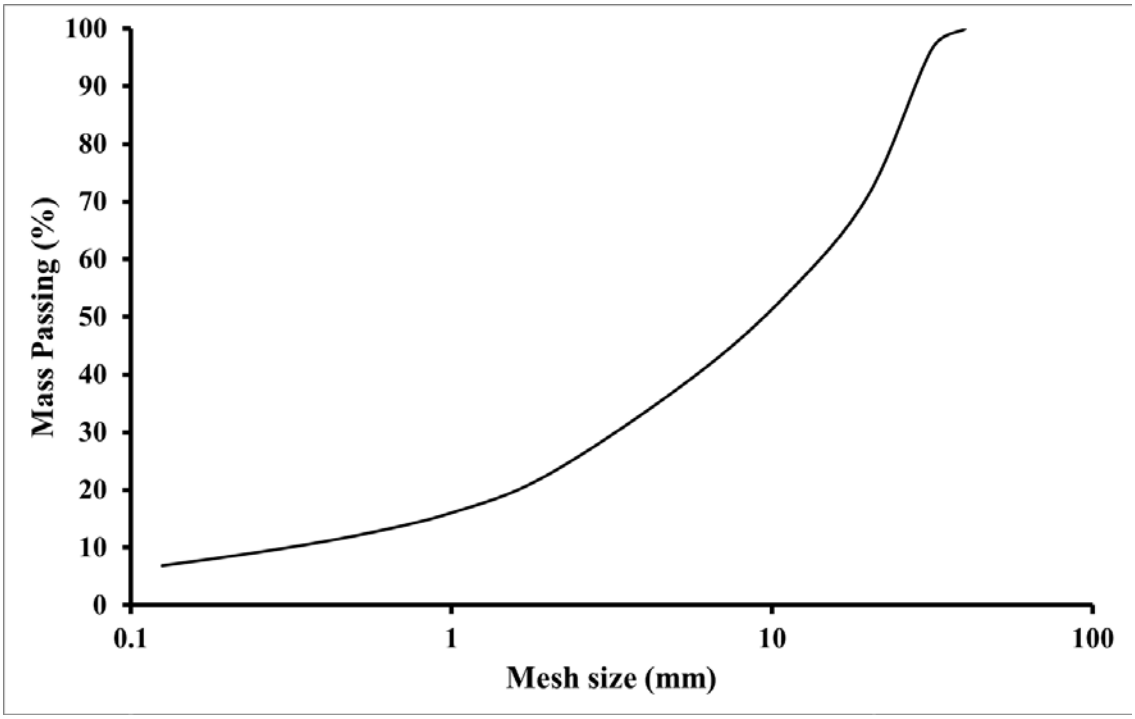

Figure 3: Average particle size distribution curve of the tested material

The tested material was weighed before placement in the mold to define the bulk density of each individual sample using the known volume in the mold. The material was placed in the mold while the telescopic system was suspended in it. After the first platform, an aluminum foil was placed to separate the first 50 mm of the material and to prevent the segregation of the fine particles.

The set-ups have been based on the applied compactive effort (CE). It has been calculated based on equation (1).

$$\text{Compactive effort} = \frac{(\text{no. of blows}) \times (\text{no. of layers}) \times (\text{weight of drop hammer}) \times (\text{drop height})}{\text{volume of material}} \quad (1)$$

The number of blows and the number of layers can be omitted since there is only one blow and one layer. The weight of the drop hammer is 35.5 kg and the volume of the material is 0.021 m^3. The drop height is defined by the impact velocity, so it is replaced by the equivalent drop height.

Results

A series of tests was performed under different compactive efforts and conditions as shown in Table 1. The number of tests was set to be at least 5 tests per set-up. However, in some cases more tests were performed for validation. The differences of the compactive efforts between dry and wet conditions are due to fresh elastic cords installed on the machine to maintain similar impact velocities.

Table 1: Test matrix of the impact tests.

Set-up/Test Classification	Impact velocity (m/s)	Compactive effort (kN-m/m^3)	Condition	No of tests
Low	5.08 ± 0.38	22 ± 0.1	dry	5
Medium	8.18 ± 1.38	56 ± 1.6	dry	5
High	12.08 ± 2.40	123 ± 4.8	dry	10
Low	5.41 ± 0.32	25 ± 0.8	wet	10
Medium	8.87 ± 0.16	66 ± 2.1	wet	5
High	10.83 ± 0.45	99 ± 0.17	wet	8

Dry material

Figures 4 and 5 show the density change at the location of the sensors as well as the compaction at the same points. The presented dynamic and static results of the compaction and densities at the measuring points were averaged over all the tests in each set-up. The dynamic results consider the maximum displacement calculated from the signals from the accelerometers. The presented results from the accelerometers are from a single test and were characteristic examples of the recordings to demonstrate the applied pulse form as well as the stress magnitude of the different applied compactive efforts. In general, the dynamic measurements showed larger dispersion than the static measurements. The recordings from the drop hammer showed the largest dispersion. This can be explained by several factors such as the drop hammer bouncing on the tested material, the progressive increased number of contact points between the drop hammer and the tested material, crushing, sliding and rotation of individual particles which are in contact

with the drop hammer. These factors might have introduced a bias in the data. In some tests, extreme values have been observed due to bouncing. However, this effect has been considered in the analysis of the results from the dynamic measurements by applying a low-pass filter (5 kHz). The dynamic measurements include the elastic and plastic deformation of the tested material, while the static measurements show only the residual deformation of the tested material.

Figure 4 shows the average compaction of the different tested samples. It includes the dynamic and static measurements at the location of the sensors. The dynamic measurements gave larger compaction (>50 %) than the static measurements (< 50 %). This result is as expected since the dynamic measurements consider the maximum deformation while static measurements considered the residual deformation.

The next set of measurements were taken at 50 mm below the surface of the tested material, the dispersion of the measurements is significantly smaller than the recordings from the accelerometer installed on the drop hammer. The bounce at this level and at the level below (150 mm from the surface of the tested material) is limited. The measured compaction at this level (50 mm) varies between 3.2 and 12.2 % and for the level below it varies between 0.5 and 4.3 %.

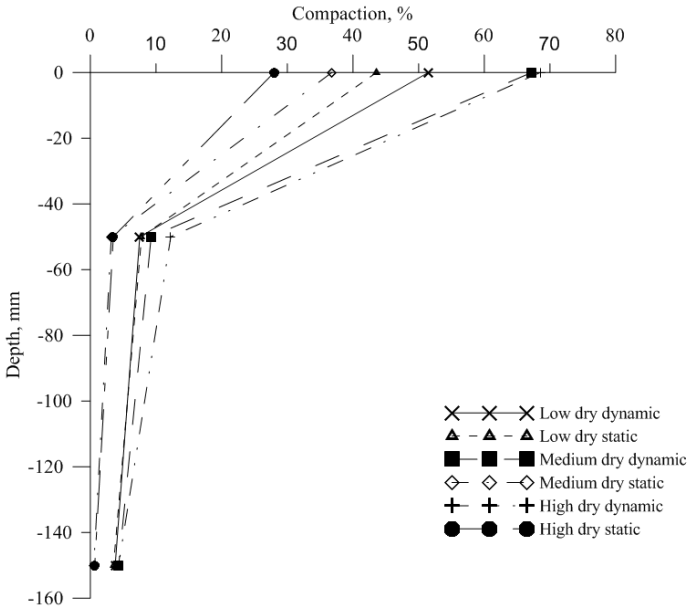

Figure 4: Compaction results from the impact tests at different set-ups for dry conditions

The magnitude of the densities from the dynamic measurements of tests with medium and high CE seems were exaggerated. The densities calculated using the static approach show that the impact with medium compactive effort densifies the tested material more than the higher and lower compactive efforts.

At the two levels below the surface of the tested material, the change in density seems less than for the first 50 mm of the material. For 50 mm and 150 mm below the surface, the density varies from 1709 to 1771 kg/m^3 and from 1677 to 1737 kg/m^3, respectively.

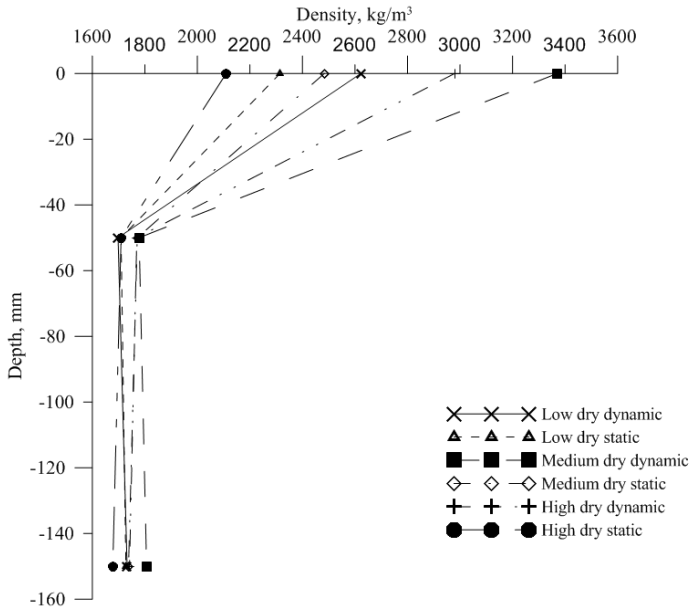

Figure 5: Density results from the impact tests at different set-ups for dry conditions

The impact duration is the time span which is required for the drop hammer to decelerate from the maximum (impact) velocity to zero. It has been calculated from the point where the velocity abruptly changes slope, i.e. from the maximum velocity (impact velocity) down to zero. As shown in Table 2 is not constant among the different set-ups. The values in Table 2 are the average of the impact duration for all tests with each set-up.

Table 2: Impact duration of drop hammer of the different set-ups

Set-up	Impact duration (ms)
Low	12.0
Medium	9.7
High	8.3

Validation tests have shown that there is no difference in particle size distribution below the first 50 mm of the tested material. Therefore, only the first 50 mm of the tested material was sieved. Moreover, the aluminum foil kept the fine particles within this 50 mm section of the tested material. The tested material at the high compactive effort showed a minor difference in particle size distribution as shown in Figure 6. Similar observation was made from visual inspection of the tested material, only some particle edges were broken, probably due to direct impact of the drop hammer on them. For the set-ups with lower compactive effort there were no measurable changes in particle size distribution.

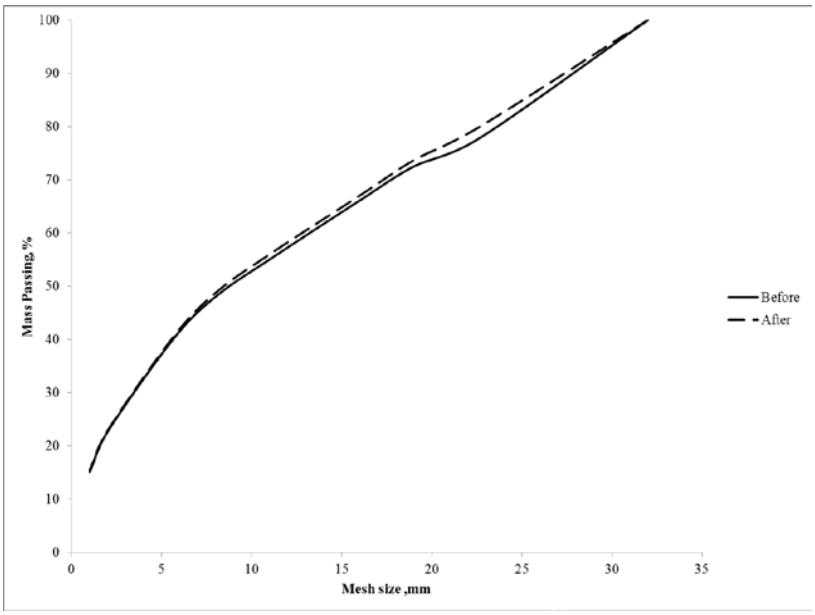

Figure 6: Average particle size distribution results before and after impact for dry conditions for high compaction effort

The recorded accelerations were used to calculate the level of impact stress using the Newton's second law of motion (2).

$$\sigma(t) = \frac{F(t)}{A} = \frac{m \cdot a(t)}{A} \tag{2}$$

where,

$\sigma(t)$ is the applied stress during the impact, A is the cross-sectional area of the drop hammer (contact area between the hammer and the material), m is the mass of the drop hammer and $\alpha(t)$ is the deceleration of the drop hammer with respect to time.

Figure 7 to Figure 9 show the stress level for the different set-ups as calculated for each sensor. The figures show characteristic recordings from the accelerometers at the different locations. The signal from the drop hammer contains high frequency components which were caused by the direct contact of the drop hammer with the surface of the tested material. There was also a contribution of high frequencies from the friction between the metal parts of the impact machine. In more details, during the first moments of the impact the surface of the drop hammer pushes down individual particles causing internal friction and frictional sliding relative to the drop hammer, eventually these high frequencies are recorded by the accelerometer.

A low pass filter (5 kHz, Butterworth filter) was applied to minimize the effect of these high frequency components on the recorded signal since they do not provide information related to mass movement. Figure 7 shows the recorded pulses from the free fall impact tests. The drop hammer pulse has longer duration compared with the pulses from the two sensors within the tested material. The pulse duration decreases as the compactive effort increases.

The contact is not instantaneous over the entire surface but starts with few a contact points until full contact has been established over the whole surface. This produces low-magnitude ripples in the recorded signal with high frequency components. However, the wave propagation velocity can be calculated between the two sensors within the tested material, i.e. sensor (2) and sensor (3). The average wave propagation velocity for the free fall tests (Figure 7) is in the magnitude of 110 m/s. In the legend of the figures, platform represents the recordings from the sensor in the filling mass, i.e. 1st platform is sensor (2) in the filling mass which is 50 mm below the impact surface, and 2nd platform is sensor (3) 150 mm below the impact surface.

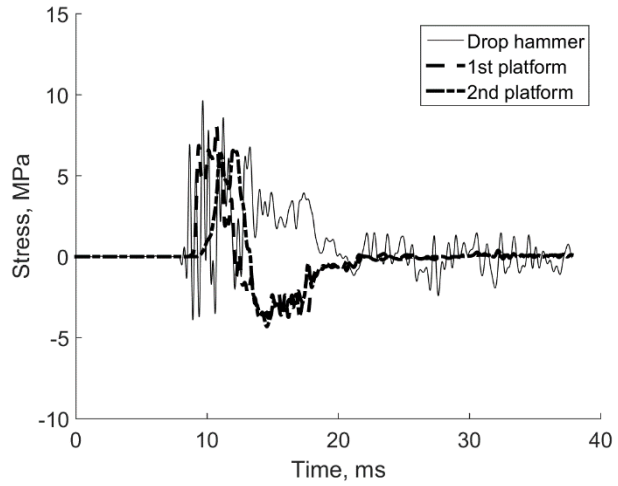

Figure 7: Impact stress for the low compactive effort for dry conditions

The average wave propagation velocity for medium CE (Figure 8) was 150 m/s and for test high CE (Figure 9) the velocity was 150 m/s. Considering this wave propagation velocity (150 m/s), the reflections of the compressive wave from the bottom of the mold are expected at 4 ms after the impact, which are visible in the signals from the accelerometers in the telescopic system after the peak (1st platform and 2nd platform).

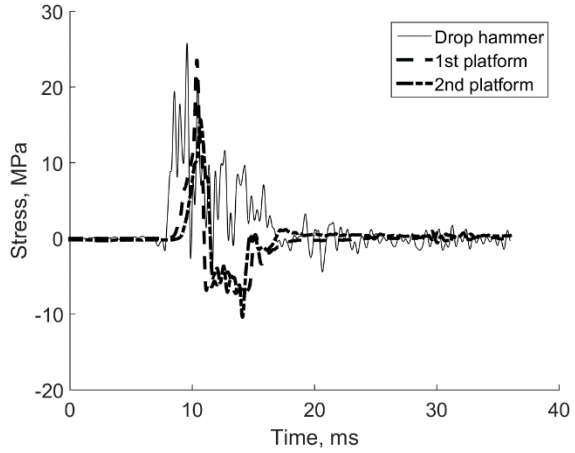

Figure 8: Impact stress for medium compactive effort for dry conditions

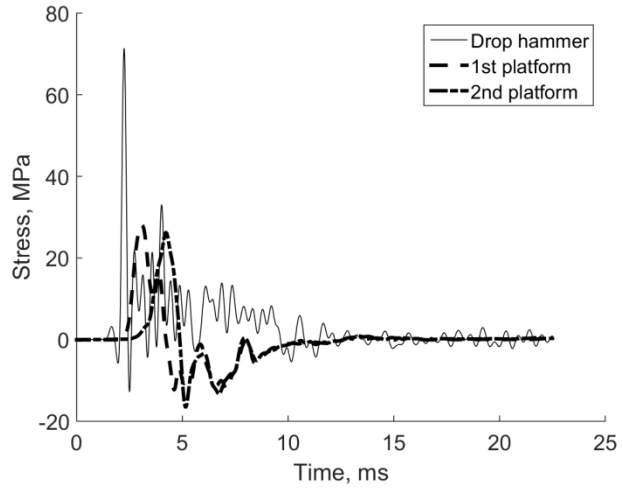

Figure 9: Impact stress for high compactive effort for dry conditions

The average changes in density of the entire sample in the mold are shown in Table 3. The density of the whole material in the mold was calculated based on the averaged residual displacement of the surface of the tested material after the impact for all the tests of each set-up. Thus, these densities originate from the static measurements. It seems that the tests with lower compactive effort show slightly larger density compared with the other two test set-ups even though the applied stresses are larger for the other set-ups. It has to be noted that the difference is not large enough to draw any solid conclusions.

Table 3: Entire material densities before and after the impact tests (initial density was 1666 kg/m^3)

	Final density (kg/m^3)
Low	1792
Medium	1771
High	1744

The last studied parameter was the angle of repose and the critical angle. After the impact test, the mold was placed on holders. The mold was titled until the material barely started rolling. The tilt angle was measured by an angle meter. The angle of repose remained constant, approximately 58^o. It should be noted that the material's angle of repose is approximately 29^o, but the effect of circularity of the mold gives an overestimation of the angle of repose. The critical angle was measured to within the range between 72^o and 79 ^{o}. The angles of repose, i.e. before and after the impact tests, have to be considered in a relative way rather than as absolute numbers.

Wet material

The next set of tests was conducted in a similar manner as the dry material tests. The only parameter that changes was the pendular water content, i.e. 2.83 % in the samples. The impact tests with the wet material showed smaller dispersion than the dry material. The compaction did

not exceed 45 % even for the dynamic measurements (Figure 10). The range of the compaction for the static measurements varies from 28 to 33 %. Additionally, for the sensors within the filling mass the compaction is slightly larger than that for the dry material. In this case, for the two positions of the sensors, it varies from 5.4 to 7 % for the sensor 50 mm and 6.8 to 8.8 % for the sensor 150 mm below the surface of the tested material. The results indicate that even minor water content in the sample influences the compaction in terms of magnitude and depth.

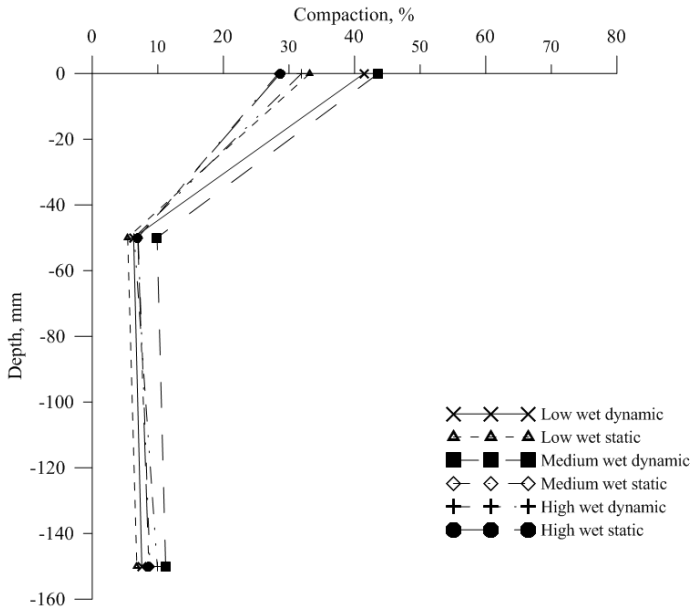

Figure 10: Compaction results from the impact tests at different set-ups for wet conditions

The density calculations seem to follow a similar pattern as the compaction calculations for the drop hammer. The density range of the first 50 mm varies from 2322 to 2489 kg/m^3, for the next 100 mm of the tested material the density varies from 1757 to 1787 kg/m^3 and from the last part of the tested material, i.e. the material between sensor (3) and the bottom of the mold, the density varies from 1783 to 1823 kg/m^3. The extent of the densification seems larger for the wet material than for the dry material. A first indication of the behavior of the tested material is that the pendular water might act as lubrication in between the particles which results in a reduction of the friction coefficient and allows larger movement of the particles.

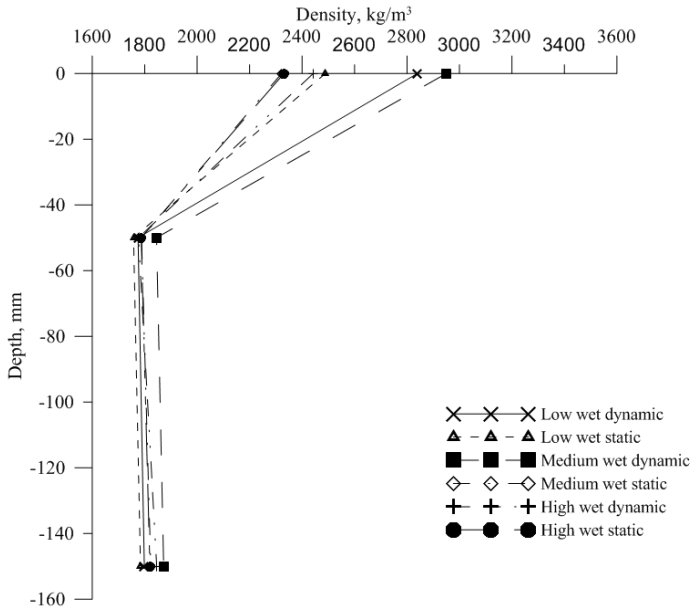

Figure 11: Density results from the impact tests at different set-ups for wet conditions

The impact duration varies from 15.2 to 10.8 ms for the different set-ups from low to high compactive effort, as shown in Table 4. The pulse duration for the wet material is longer than that of the dry material. This might be explained by the fact that the tested material was less stiff than the dry material.

Table 4: Impact duration for wet conditions

Set-up	Impact duration (ms)
Low	15.2
Medium	12.1
High	10.8

Figures 12-14 show the behavior of the wet tested material during impact. It should be noted that the figures show the typical recordings from an impact test and they do not precisely agree with the presented average stress values. The average stress level for the low CE tests (Figure 12) was approximately 6 MPa for the first and second sensor in the tested material. As in the dry material, there were some problems to identify the main pulse from the drop hammer to calculate the wave propagation velocity in the material. However, as in the case of the dry material, the wave propagation velocity between the two sensors, i.e. sensor (2) and sensor (3), for the low and medium CE tests within the filling material can be calculated. The average calculated velocity was 130 m/s.

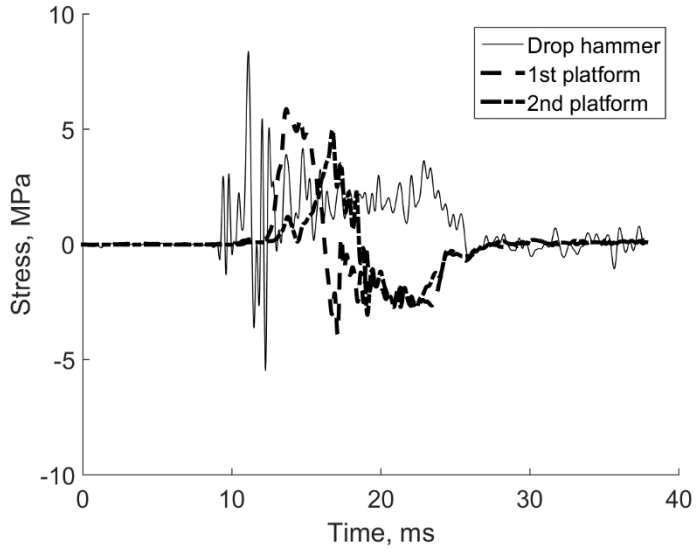

Figure 12: Impact stress for the low compactive effort for wet conditions

For tests with medium CE (Figure 13) the average stress level was approximately 21 MPa for the first and 18 MPa for the second sensor within the tested material. For the high compactive effort, the average applied stress was 35 and 26 MPa for the first and the second sensor, respectively. The reaction of the tested material is shown in Figure 14.

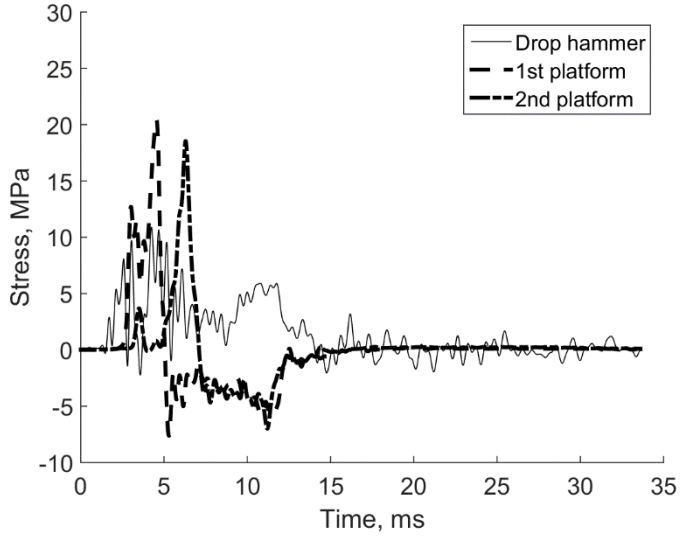

Figure 13: Impact stress for medium compactive effort for wet conditions

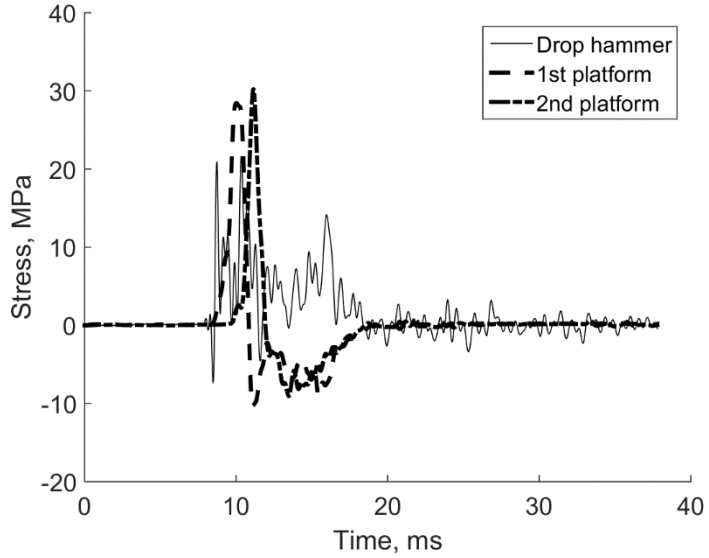

Figure 14: Impact stress for high compactive effort for wet conditions

Regardless of the set-up, the effect of impact on the particle size distribution of the material is minor. There was no noticeable change in particle size distribution at low or medium CE, and at high CE there is only a difference when the mesh is finer than 8 mm. Figure 15 shows the average particle distribution for all high CE tests, where the percentage of material passing the finest mesh sizes is greater following the tests. The reason only the finest mesh sizes were affected is because the impact tests did not break large particles generally, but only affected the edges of these particles, resulting in higher sphericity. The location of these particles was on the surface of the tested material, which indicates that these particles were in direct contact with the drop hammer. Further observations after the impact tests revealed that the coarse particles at the surface have been buried due to impact.

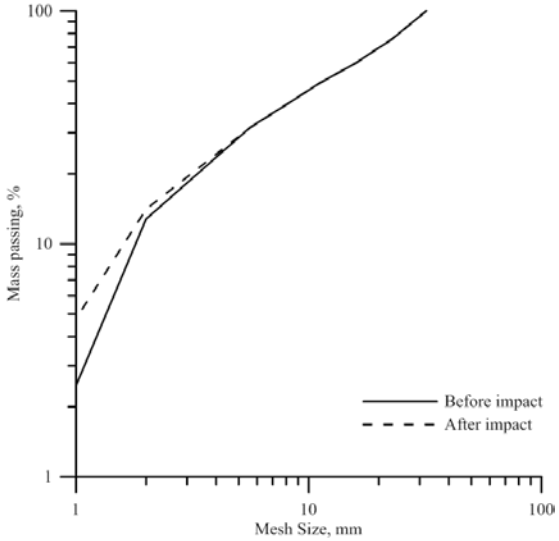

Figure 15: The average particle size distribution results before and after impact for wet conditions and high CE

The overall change in density of the entire material in the mold and for all the set-ups is shown in Table 5. The density of this material is larger than the final density of the dry material. Thus, the water, even in pendular state, has a significant effect on the final density. As mentioned before, it has been observed that the pendular water acts as lubrication in the tested material which indicates that larger deformations can be achieved.

Table 5: Densities for wet conditions (initial density was 1662 kg/m^3)

	Final density (kg/m^3)
Low	1862
Medium	1878
High	1875

Similarly to as in dry material, the angle of repose for the wet material was measured. The angle of repose before the impact tests was 67^o, 63.8^o and 63^o for low, medium and high compactive efforts, respectively. The variation in the angle of repose before the impact tests was due to variation of the material. Again, there was influence of the circularity of the mold. After the impact the impact tests the critical angle were 84^o, 89.6^o and 82^o for the same test set-ups. The larger angle of repose for the wet material indicates that the mobility of the material has been affected by the content of pendular water. Visual observations indicated a wall formation of the compacted material, but it was stable only for a very short period (minutes) and very sensitive even to minor vibrations.

Discussion

The two conditions, dry and wet, have a fundamental difference which can affect the mechanical properties of the material. The dry material is cohesionless but the wet material, even in pendular state, has cohesion. This influences the angle of repose, introduces tensile strength due to water bridges at the contact points and causes agglomeration which creates clusters of particles increasing their sphericity.

As can be seen from the results, the critical angle was not significantly affected by the compactive effort but was affected by the condition of the material. The wet material gives larger angles of repose and critical angles than the dry material. Similar observations have been made by Mitarai & Nori, (2006), Samadani & Kudrolli, (2001), Nowak, et al., (2005) and Herminghaus, (2005). It can be explained by the fact that water tends to build small capillary bridges between the particles which exert attractive forces between the particles.

In some tests with the wet material, there was a wall formation when the mold was tilted after the impact test whereas in dry material, this wall formation was not observed. This might be directly connected with the larger critical angles which indicate a potential particle interlocking and increase of the number of contact points between individual particles which results in a more stable structure.

The presence of water in the material also increases mobility due to lubrication action between the particles. This indicates that the friction coefficient between the particles changes compared to the dry material. This effect can be observed by the difference in the final compaction and final density of the material. In the case of the wet material, the influenced zone, i.e. the extent of the compaction zone, is deeper than for the dry material (Figure 16). Thus, the influenced zone is more dependent on the material conditions than the compactive effort. Additionally, it has to be noted that there is only one degree of freedom since the material can move only along its vertical axis due to the confinement of the mold. The lower compactive efforts (medium and low) for both conditions (dry and wet) gave the largest compaction at the surface of the material, considering only the static measurements.

The duration of the impact represents the required time for the kinetic energy to be transferred from the drop hammer to the tested material. It was varied between the different set-ups and conditions. In general, as the compactive effort increases, the duration of the impact becomes shorter. The duration for the dry material is shorter than that for the wet material. This can be explained by the fact that the wet material has a lower friction coefficient. The particles can thus be moved longer distances in the wet material than in the dry material. It is also shown by the impact duration of the wet material which is 2-3 ms greater than in the dry material.

A comparison of the peak stresses between the dry and wet material shows that the stress level is higher in the dry material than that in the wet material. This can be related with the material properties. It appears to be that the wet material is less stiff than the dry material. It should be noted that the amount of energy transferred is similar for both material conditions. A combination of the stress level and the duration of the impact can explain the larger compaction exhibited by the wet material as well as the depth of the influence zone by the impact.

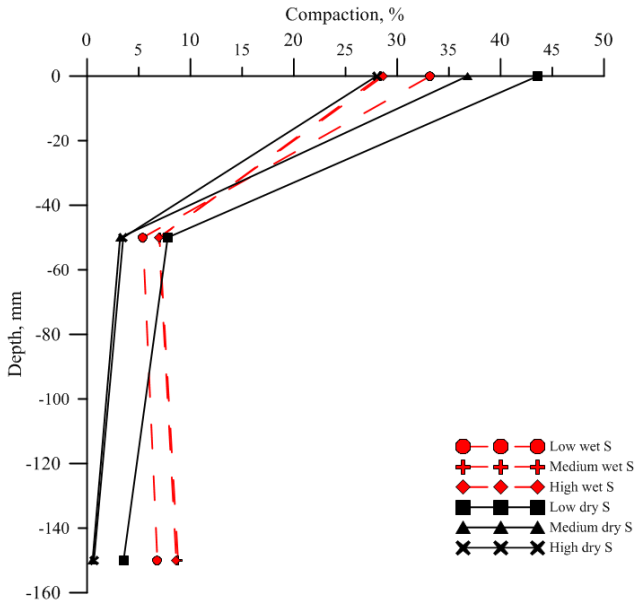

Figure 16: Comparison of compaction from static measurements

The literature is very limited regarding the comparison of the impact duration between dry and wet granular materials. Several studies, e.g. Chow, et al., (1990), Mayne & Jones, (1983) and Poran, et al., (1991), have been performed in the past to evaluate compaction by means of deceleration measurements. The pulse forms from the above studies are very similar to those that have been recorded in this study; it has a triangular shape followed by a bounce of the hammer on the surface of the material and reflections of the compressive wave. The difference in magnitude and frequency components is caused by of the nature of the tested material, in most cases, it is a type of sand, in this study, the tested material is coarse-grained crushed aggregate. This material can produce high frequency components since the particle size is large enough to scratch or slide on the surface of the drop hammer.

Since compaction and density are directly related, the change in density also causes a change in porosity of the tested material. The initial density is approximately 1666 kg/m^3, the final densities are in the order of 1770 kg/m^3 and 1870 kg/m^3 for the dry and wet material, respectively. Hence the porosity changes from 36.8 % (initial porosity) to 32.9 and 29 % for the two cases, i.e. dry and wet material. The decrease in porosity increases the number of contact points which is reflected in the increase of critical angle.

Another studied parameter was the particle size distribution changes due to impact of the drop hammer on the surface of the tested material. Based on the presented results there was no significant change in particle size distribution, although edges from particles were broken, especially at the particles on the surface of the material which were in direct contact with the drop hammer. This observation is valid for both cases, i.e. dry and wet material. The low and medium compactive effort did not show any measurable change in particle size distribution.

Conclusions

The results of this study showed that the water content, even in pendular state, in a coarse-grained material has a significant effect on its physical properties, i.e. compressibility, stability and density. The compressibility is increased since the pendular water acts as lubricant in between the particles leading to a reduction of the friction coefficient and increases mobility which decreases the porosity of the tested material. However, the stability of the material is increased as shown by the increase in the critical angles which indicates larger number of contact points in between the particles and the larger number of capillary bridges which contribute to stability of the impacted material. The influenced depth of the compacted material is dependent on the condition of the material, dry or wet, rather than the compactive effort.

The peak stress and the impact duration are dependent on the condition of the material; dry material gave shorter impact duration and higher peak stresses were observed in the dry material than the wet material.

Only a minor change in particle size distribution was observed for dry and wet material for the larger compactive effort. There was no measurable change in particle size distribution for low and medium compactive efforts. Additionally, no change in particle size distribution was observed below 50 mm from the surface of the impacted material.

Acknowledgements

The authors thank the Hjalmar Lundbohm Research Centre (HLRC), a research foundation at Luleå University of Technology, endowed by LKAB for its financial support of the titled project "Improved understanding of sublevel blasting: Determination of the extent of the compacted zone, its properties and the effects on caving". Swebrec and LKAB are also thanked for partially financing this project.

References

[1] Menard, L. & Broise, Y., 1975. Theoretical and practical aspects of dynamic consolidation. Geotechnique, 25(1), pp. 3-18.

[2] Jessberger, H. L. & Beine, R. A., 1981. Heavy tamping: theoretical and practical aspects. Stockholm, Publ Rotterdam: A. A. Balkema, pp. 695-699.

[3] Mayne, P. W. & Jones, J. S., 1983. Impact stresses during dynamic compaction. Journal of Geotechnical and Geoenvironmental Engineering, 109(10), pp. 1342-1346.

[4] Womac, A. R. et al., 1989. Measuring dynamic response of soil subjected to impact loading. Soil & Tillage Research, Volume 14, pp. 25-38.

[5] Poran, C. J., Rodriguez, J. A. & Heh, K. S., 1991. Impact response of granular soils. St. Louis, Missouri, University of Missouri--Rolla.

[6] Thilakasiri, H. S. et al., 1996. Investigation of impact stresses induced in laboratory dynamic compaction of soft soils. Int. J. Numer. Anal. Meth. Geomech., Volume 20, pp. 753-767.

[7] Oshima, A. & Takada, N., 1998. Evaluation of compacted area of heavy tamping by cone point resistance. Rotterdam, Balkema, pp. 813-818.

[8] Merrifield, C. M. & Davies, M. C. R., 2000. A study of low-energy dynamic compaction: field trials and centrifuge modelling. Geotechnique , 50(6), pp. 675-681.

[9] Gu, Q. & Lee, F. H., 2002. Ground response to dynamic compaction of dry sand. Geotechnique, 52(7), pp. 481-493.

[10] Jafarzadeh, F., 2006. Dynamic compaction method in physical model tests. Scientia Iranica, 13(2), pp. 187-192.

[11] Scott, R. A. & Pearce, R. W., 1975. Soil compaction by impact. Géotechnique, 25(1), pp. 19-30.

[12] Chow, Y. K., Yong, D. M., Yong, K. Y. & Lee, S. L., 1992. Dynamic compaction analysis. Journal of Geotechnical and Geoenvironmental Engineering, 118(8), pp. 1141-1157.

[13] Chow, Y. K., Yong, D. M., Yong, K. Y. & Lee, S. L., 1990. Monitoring of dynamic compaction by deceleration measurements. Computers and Geotechnics, Volume 10, pp. 189-209.

[14] ASTM D2487-11, 2011. Standard practice for classification of soils for engineering purposes (Unified soil classification system). West Conshohocken: American Society for Testing and Material .

[15] Petropoulos, N., Mihaylov, D., Johansson, D. & Nordlund E., 2017. A suggested method for the study of crushed aggregate response to dynamic compaction. Electronic Journal of Geotechnical Engineering, 22(02), pp. 387-406.

[16] ASTM D2216-10, 2010. Standard test methods for laboratory determination of water (moisture) content of soil and rock by mass. West Conshohocken: American Society for Testing and Materials.

[17] ASTM C136/C136M-14, 2014. Standard test method for sieve analysis of fine and coarse aggregates. West Conshohocken: American Society for Testing and Materials.

[18] Newitt, D. W. & Conwey-Jones, J. M., 1958. A contribution to the Theory and practise of granulation. Transaction, Institution of Chemical Eng., Volume 36, pp. 422-442.

[19] Mitarai, N. & Nori, F., 2006. Wet granular materials. Advances in Physics, 55(1-2), pp. 1-45.

[20] Samadani, A. & Kudrolli, A., 2001. Angle of repose and segragation in cohesive granular material. Physical Review, Volume 64, p. 050301.

[21] Nowak, S., Sadamani, A. & Kudrolli, A., 2005. Maximum angle of stability of a wet granular pile. Nature Physics, Volume 1.

[22] Herminghaus, S., 2005. Dynamics of wet grnaular matter. Advances in Physics, 54(3), pp. 221-261.